DOI: 10.1002/chem.201001352

Dynamic Octopus Amphiphiles as Powerful Activators of DNA Transporters: Differential Fragrance Sensing and Beyond

Javier Montenegro, Pauline Bonvin, Toshihide Takeuchi, and Stefan Matile*[a]

Abstract: We report the design, synthesis and evaluation of dynamic "octopus" amphiphiles with emphasis on their efficiency as activators in synthetic membrane-based sensing systems. Previously, we found that the in situ treatment of charged hydrazides with hydrophobic aldehydes or ketones gives amphiphilic counterion activators of polyion transporters in lipid bilayers, and that their efficiency increases with the number of their hydrophobic tails. Herein, we expand this series to amphiphiles with one cationic head (guanidinium or ammonium) and four exchangeable hydrophobic tails. These results, with the highest number of tails reported to date, confirm that dynamic octopus amphiphiles provide access to maximal activity and selectivity. Odorants, such as muscone, carvone, or anisaldehyde are used to outline their usefulness in differential sensing systems that operate based on counterion-activated DNA transporters in fluorogenic vesicles. The enhanced ability of octopus amphiphiles to enable the discrimination of enantiomers as well as that of otherwise intractable *ortho*, *meta*, and *para* isomers and short cyclo-/alkyl tails is demonstrated. These findings identify dynamic octopus amphiphiles as being promising for application to differential sensing, "fragrant" cellular uptake, and slow release.

Keywords: amphiphiles · DNA · membranes · sensors · supramolecular chemistry

Introduction

Olfactory sensing systems operate in lipid bilayer membranes.[1] However, the creation of synthetic sensing systems that work in the same way as in nature has been troublesome.[2–4] The synthesis of transport systems[5–17] that respond to chemical stimulation was the first key step to achieve this goal.[18–20] In sensing systems, these stimuli-responsive transporters function as signal transducers. Their combination with enzymes as signal generators[21,22] afforded the first functional sensors that are operational in complex matrices from the supermarket to hospitals.[23,24] General applicability as multianalyte sensing systems, finally, became possible with the introduction of reactive in-/activators as bifunctional molecules that can, on the one hand, covalently capture the product of enzymatic signal generation and, on the other hand, modulate the activity of the synthetic transport system.[24,25] However, synthetic sensing systems in bilayer membranes that operate with enzymes (or DNA aptamers)[26] as signal generators will never reach the sensing power of mammalian olfactory systems, where 350 receptors suffice to sense more than 10000 odorants.[1]

To get there, we have recently introduced pattern recognition to synthetic systems that work in lipid bilayer membranes (Figure 1).[27] In pattern recognition or "differential" sensing approaches, single analytes are identified and quantified not from molecular recognition by one specific sensor but as a unique composite response or fingerprint.[28–40] Pattern recognition is attractive for signal generation because promiscuous behavior of individual sensors is not only tolerated but preferable, and an infinite number of analytes can be detected with a relatively small number of individual sensing units. Pattern-recognition approaches have been applied previously to several chemosensor systems[28–46] that operate with indicator displacement assays, stimuli-responsive dyes, polymer absorption, or electrochemical reactions.[28–40] Topics addressed with differential sensing include not only analyte families, such as anions, sugars, amino acids, or nucleotides but also challenges, such as the discrimination of stereoisomers or the creation of electronic, colorimetric or fluorescent artificial tongues and noses.

[a] Dr. J. Montenegro, P. Bonvin, Dr. T. Takeuchi, Prof. S. Matile
Department of Organic Chemistry
University of Geneva, Geneva, Switzerland
Fax: (+41) 22 379 3215
E-mail: stefan.matile@unige.ch

Supporting information for this article is available on the WWW under http://dx.doi.org/10.1002/chem201002352.

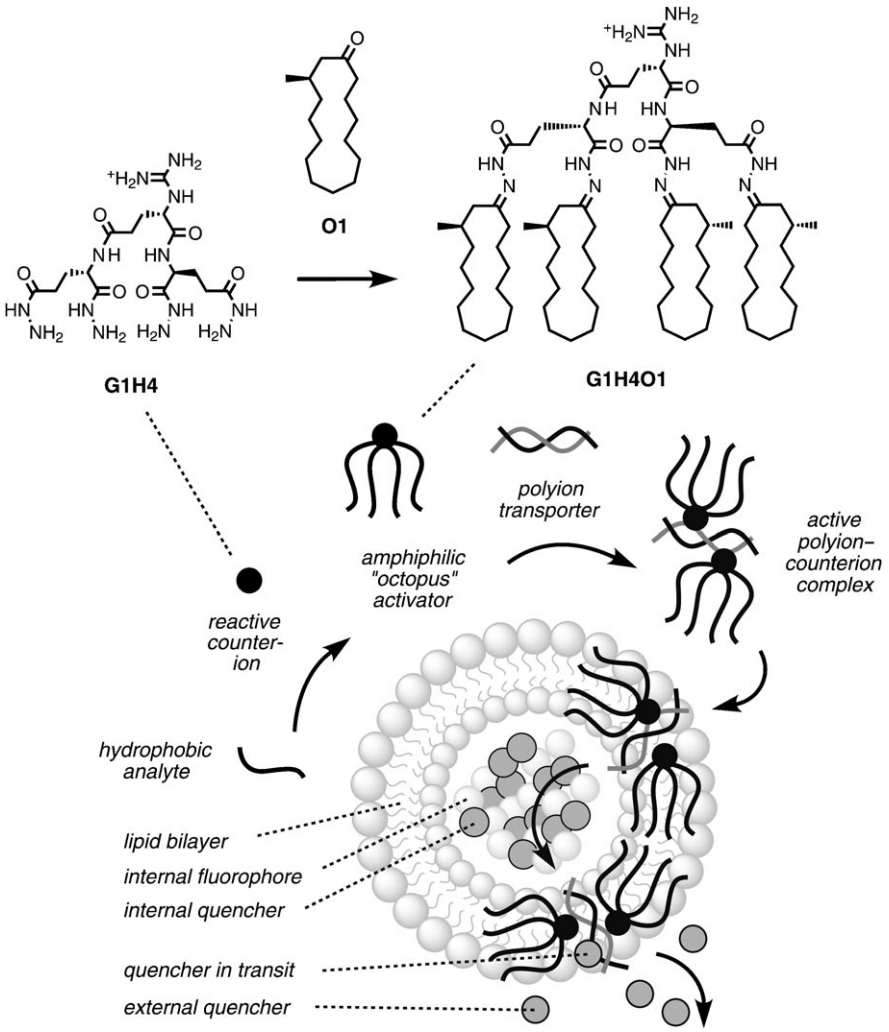

Figure 1. Scheme for synthetic sensing systems in fluorogenic vesicles. Hydrophobic analytes (e.g., muscone **O1**) are covalently captured by hydrophilic countercations (e.g., tetrahydrazides **G1H4**) to give four-tailed octopus amphiphiles (e.g., **G1H4O1**) that can activate polyanions (e.g., ctDNA) as transporters in lipid bilayer membranes. Transporter activation by hydrophobic analytes is reported as increase in the emission of internal anionic fluorophores in response to the export of cationic quenchers (or both probes).

Differential sensing has not been applied to synthetic systems that operate in lipid bilayers because the number of available cross-responsive sensor components has been insufficient.[3,4] To overcome this limitation, we have considered the following sensing scheme.[27] Hydrophobic analytes, otherwise undetectable with membrane-based sensing systems, are first covalently captured by reactive hydrophilic cations (Figure 1). The resulting amphiphiles can act as countercation activators for polyanions and generate active polyion–counterion transport systems. Their change in activity caused by the hydrophobic analyte can be monitored by several different methods. Arguably the simplest technique is to follow fluorescent recovery while cationic quenchers (and/or anionic fluorophores) are carried out of fluorogenic vesicles.

For pattern generation, a small collection of reactive counterions **G1H1**–**G1H3** and **A1H1**–**A1H3** has been designed, synthesized, and used to produce the unique fingerprints needed for differential sensing.[27] Incubation of analytes with different reactive counterions produces a small collection of in-/activators of synthetic transport systems (Figure 1). From the fluorescent response to increasing activator concentrations, characteristics, such as the maximum normalized response as determined after 190 s (Y_{MAX}), the effective concentration to reach 50 % of this maximal activity (EC_{50}), or the Hill coefficient (n) are extracted to generate analyte specific patterns. These multidimensional patterns are then subjected to principal component analysis (PCA) and hierarchical cluster analysis (HCA) to convert n-dimensional space into three-dimensional PC space and 2D dendrograms, respectively.

This approach to differential sensing systems that work like olfactory systems in lipid bilayer membranes has been exemplified with hydrophobic analytes containing a ketone or an aldehyde, such as odorants **O1**–**O13** (Scheme 1).[27] Without modification, these analytes are essentially undetectable with most synthetic sensing systems that operate in lipid bilayer membranes. However, their incubation with cations **G1H1**–**G1H3** and **A1H1**–**A1H3** that contain at least one hydrazide gives hydrazones, such as **G1H1O1**–**G1H3O13**, and **A1H1O1**–**A1H3O13**, which in turn can activate polyanions, such as calf thymus DNA (ctDNA) as cation transporter in fluorogenic vesicles (Figures 1 and Scheme 1). This new sensing system can differentiate between enantiomers (e.g., enantioenriched (*R*)-(−)-muscone **O1** (61 % *ee*) versus racemic muscone **O2**, *R*-(−)-carvone **O9** (caraway) versus *S*-(+)-carvone **O10** (spearmint)), *cis*–*trans* isomers, single atom homologues (e.g., **O5**–**O8**) or perfumes, as examples of more complex matrices used in daily life.

Sensing sensitivity is best with long, linear, or branched alkyl or aryl tails including **O6**–**O8**, whereas shorter alkyl or aryl tails, such as **O3**–**O5**, **O11**–**O13**, and cyclic ketones, such as **O1**–**O2**, **O9**–**O10**, are more difficult to detect under standard conditions. However, such analytes could be sensed as competitive inhibitors of other more easily detectable odorants in inverse detection schemes.

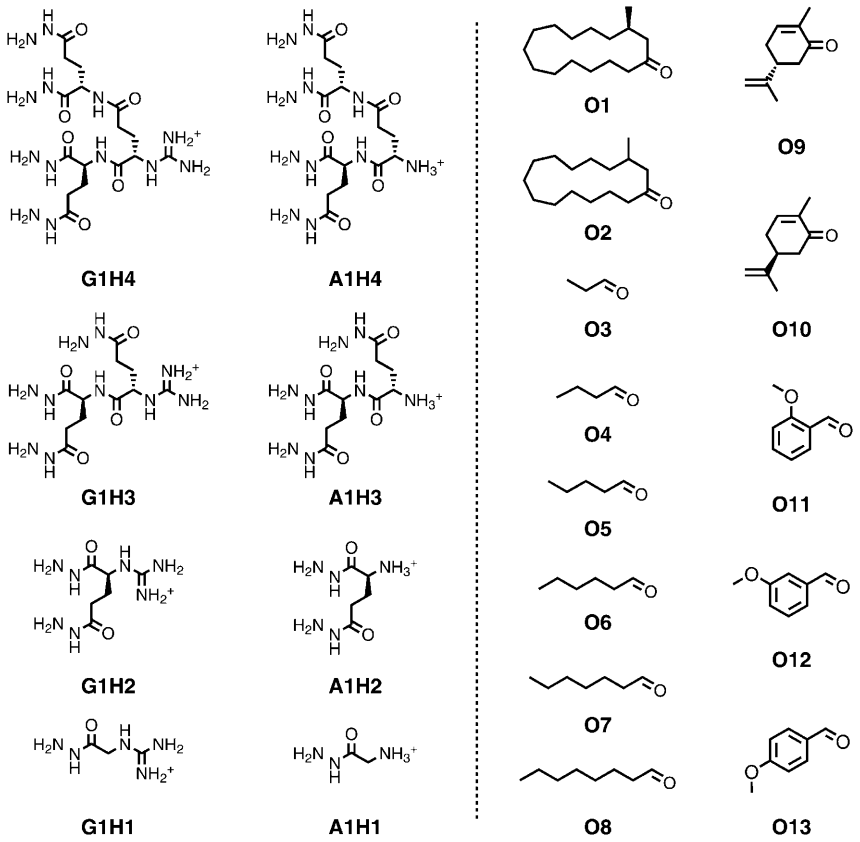

Scheme 1. New reactive counterions **A1H4** and **G1H4** for differential sensing systems in fluorogenic vesicles with odorant analytes that are not well detectable with the previously reported **A1H1**–**A1H3** and **G1H1**–**G1H3**, including enantioenriched (*R*)-(−)-muscone **O1** (61% *ee*), racemic (±)-muscone **O2**, (*R*)-(−)-carvone **O9** (caraway), (*S*)-(+)-carvone **O10** (spearmint), *ortho*-, *meta*-, and *para*-anisaldehydes **O11**–**O13**, or butanal **O4**.

As far as reactive cations **G1H1**–**G1H3** and **A1H1**–**A1H3** are concerned, guanidinium cations have been better than ammonium cations, and efficiencies of signal generation (e.g., Y_{MAX}/EC_{50}) increased with increasing numbers of hydrazides. This observation called for the synthesis of charged peptide dendrons[47–51] as modular scaffolds that offer multiple hydrazides to attach hydrophobic aldehydes and thus produce "octopus" amphiphiles with one head and many sticky tails ("tentacles"). Herein, we report the modular synthesis of dendrons **A1H4** and **G1H4**, and show that most of the guanidinium amphiphiles **G1H4O1**–**G1H4O13** obtained from incubation with odorants **O1**–**O13** can activate DNA transporters in bilayer membranes with unprecedented efficiency. This result is of interest not only to expand the scope of synthetic differential sensing systems in lipid bilayer membranes but also for biological applications, such as cellular uptake.[49–54]

Results and Discussion

Synthesis: Synthetic sensing systems that can really be of use in practice are either very straightforward to prepare or have exceptional characteristics that overcompensate the cost of more demanding synthetic efforts. The synthesis route to multihydrazide counterions was designed as a modular approach based on routine peptide chemistry to maximize user-friendly simplicity. Tetrahydrazide **G1H4** was synthesized from *Z*-protected glutamate **1** in six steps, overall, with 20% total yield (unoptimized) and under mild conditions (Scheme 2). Namely, treatment of **1** with glutamate diester **2** afforded the desired tetravalent scaffold in a single step. The obtained tetraester **3** was treated with hydrazine to give nearly intractable tetrahydrazides. However, conversion of the crude product with Boc-anhydride readily afforded the Boc-protected tetrahydrazides **4**, and the desired peptide dendron[47–51] scaffold was purified without problems under standard conditions. Selective *Z* removal by hydrogenolysis gave amine **5**, which was guanidinylated with *N*,*N*′-di-Boc-1*H*-pyrazole-1-carboxamidine (**6**). Complete deprotection of the obtained tripeptide **7** under acidic conditions gave the target molecule **G1H4**. Tetrahydrazide **A1H4** with an ammonium cation in place of the guanidinium cation was obtained by deprotection of intermediate **5**.

All new compounds were optically active, and their ^{1}H NMR spectra showed no indication of epimerization. This observation was further supported by a single peak in the reverse-phase (RP) HPLC of the protected target molecule **7**.

Characterization: The activity of the new tetrahydrazide cations **G1H4** and **A1H4** was determined by comparison with the previously reported trihydrazide cations **G1H3** and **A1H3** (Scheme 1). However, the solubility of ammonium tetrahydrazide **A1H4** and most of its tetrahydrazone derivatives was insufficient to encourage meaningful in-depth characterization. In striking contrast, the solubility of the corresponding guanidinium tetrahydrazide **G1H4** and all tetrahydrazone derivatives was unproblematic. Octopus amphiphiles **G1H4O1**–**G1H4O13** were prepared individually by incubation with 2 equiv odorants **O1**–**O13** per hydrazide in DMSO for 1 h at 60 °C (Figure 1).[27] Their ability to activate polyanion transporters was explored under routine conditions with ctDNA transporters in EYPC-LUVs⊃HPTS/DPX

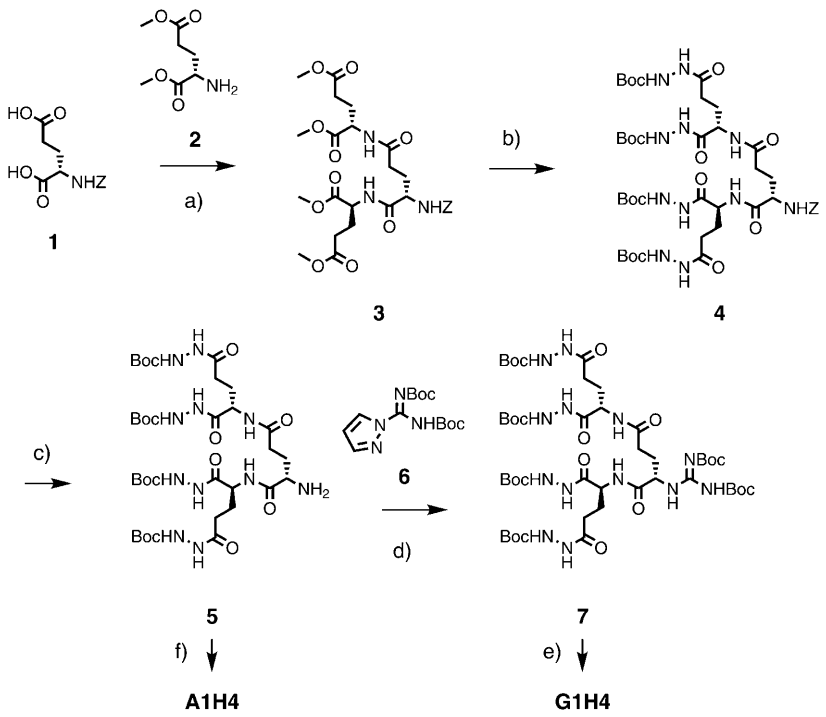

Scheme 2. a) *O*-(Benzotriazol-1-yl)tetramethyluronium hexafluorophosphate (HBTU), N,N-diethylamine (DEA), CH_2Cl_2, room temperature; b) 1. N_2H_4 monohydrate, MeOH, room temperature; 2. Boc_2O (Boc = *tert*-butyloxycarbonyl), MeCN, H_2O, room temperature, 34% (three steps); c) H_2, Pd/C, room temperature, quant; d) ethyldiisopropylamine (DIEA), MeCN, 50°C, 64%; e) 1 M HCl in Et_2O, CH_2Cl_2, reflux, 91%; f) 1 M HCl in Et_2O, CH_2Cl_2, reflux, 94%.

(egg yolk phosphatidylcholine large unilamellar vesicles loaded with the anionic fluorophore 8-hydroxy-1,3,6-pyrenetrisulfonate and the cationic quencher *p*-xylene-bis-pyridinium bromide, Figure 1). In this assay, the ability of DPX and/or HPTS to leave the vesicle is reported as fluorescence recovery independent of the mechanism of transport. However, previous controls in the U-tube have confirmed that counterion-activated DNA can act as cation carrier at low concentrations.[20]

In a typical procedure, octopus amphiphile **G1H4O8** was added as concentrated stock solution in DMSO to the stirred and thermostated suspension of fluorogenic vesicles (Figure 2). Unchanged fluorescence at this point confirmed that octopus amphiphiles **G1H4O8** alone are not active in lipid bilayer membranes. After a brief incubation period, ctDNA was added as concentrated aqueous stock solution to produce operational polyion–counterion transporters. Their ability to mediate DPX export was then followed as fluorescence recovery as a function of time. At the end of each experiment, vesicles were lysed to reach the constant final emission intensity needed for calibration. These experiments were repeated for various concentrations of octopus amphiphile **G1H4O8** at constant DNA concentration. Increasing activity with increasing concentrations of **G1H4O8** was found (Figure 2). This trend was quantified in the dose-response curve of octopus amphiphile **G1H4O8** (Figure 3a, ○).

Hill analysis of the dose-response curve gave the three fundamental characteristics describing octopus amphiphile **G1H4O8** (Figure 3a, ○, -----), that is, $EC_{50} = (3.9 \pm 0.2)$ μM, $Y_{MAX} = (62.2 \pm 1.5)$% and the Hill coefficient $n = 3.3 \pm 0.4$, reporting an informative combination of stoichiometry, stability and cooperativity of the active transport system.[55] The EC_{50} remained constantly low for octyl, heptyl, and hexyl tails in **G1H4O8** (Figure 3a, ○), **G1H4O7** (Figure 3a, □), and **G1H4O6** (Figure 3a, ▼), respectively. This poor discrimination among long alkyl tails suggests that the limit of stoichiometric binding[56] is reached and activities cannot be further improved in the given assay. The pentyl tails in octopus amphiphile **G1H4O5** produced a clearly reduced $EC_{50} = (23.8 \pm 1.5)$ μM at preserved high

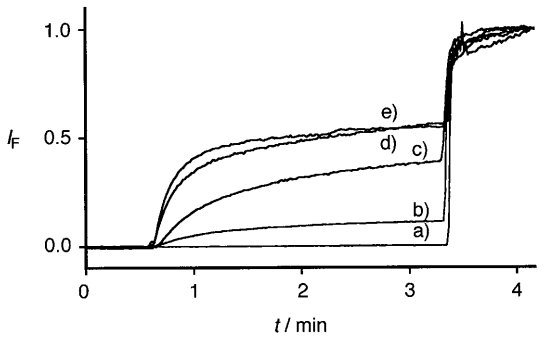

Figure 2. Changes in fractional fluorescence intensity (I_F) of HPTS (λ_{ex} = 413 nm, λ_{em} = 510 nm) during addition of **G1H4O8**: a) 1, b) 2.5, c) 5, d) 10, and e) 25 μM (final concentrations $t < 0$ s), ctDNA (1.25 μg mL^{-1} final concentration, $t = 40$ s) and Triton X-100 (0.024% final concentration, $t = 200$ s) to EYPC-LUVs⊃HPTS/DPX.

$Y_{MAX} = (60.1 \pm 3.2)$% (Figure 3a, ●). The butyl tails in **G1H4O4** remained with $EC_{50} = (63.9 \pm 2.8)$ μM detectable below the 100 μM threshold, although the Y_{MAX} dropped to a less important $Y_{MAX} = (14.9 \pm 1.0)$% (Figure 3a, ▲). **G1H4O3** was not characterized because the detection limit was reached with **G1H4O4**.

Compared to previously reported results with guanidinium amphiphiles with three (**G1H3**, Figure 3b), two (**G1H2**, Figure 3c), and one tail (**G1H1**, Figure 3d),[27] the results for the *n*-alkyl series of the new octopus amphiphile **G1H4** (Figure 3a) revealed the following clear trends. Most important-

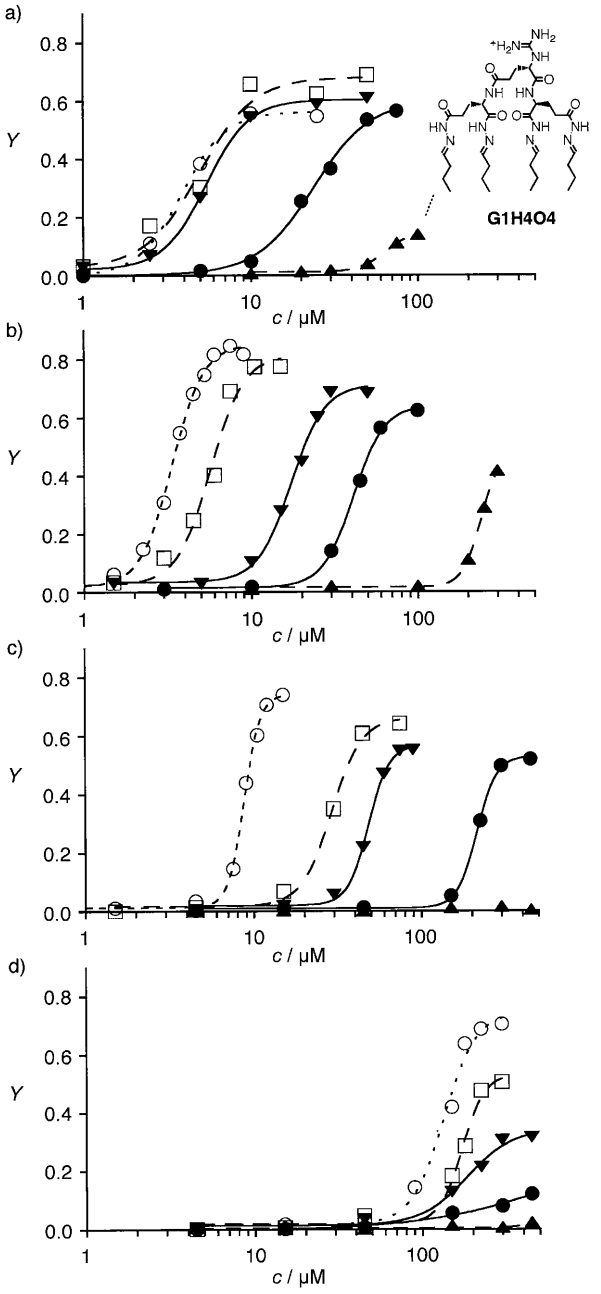

Figure 3. Dose-response curves for DNA activation by guanidinium hydrazides: a) **G1H4**, b) **G1H3**, c) **G1H2**, and d) **G1H1** after incubation with octanal **O8** (○), heptanal **O7** (□), hexanal **O6** (▼), pentanal **O5** (●), and butanal **O4** (▼). Data for **G1H3**, **G1H2**, and **G1H1** are adapted from ref. [27]; for details, compare original data for amphiphile **G1H4O8** in Figure 2 and the Supporting Information.

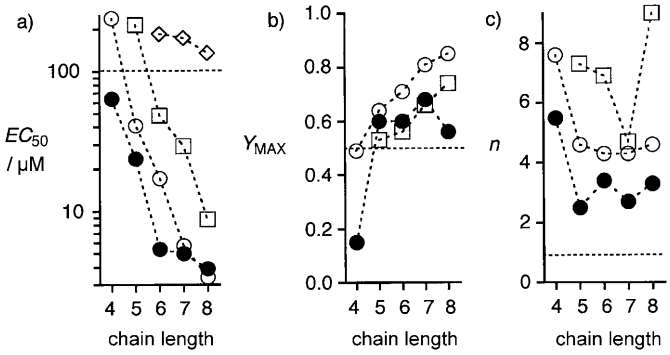

Figure 4. Dependence of: a) the effective concentration EC_{50}, b) the maximal activity (Y_{MAX}), and c) the Hill coefficient (n) of **G1H4** (●), **G1H3** (○), **G1H2** (□), and **G1H1** (◇) on the length of the n-alkyl tail of the aldehyde they are derivatized with (in number of carbons), with indication of pertinent thresholds as dotted lines ($EC_{50}=100$ μM, $Y_{MAX}=0.5$, $n=1$). Data from the Hill analysis of the curves in Figure 3.

ly, EC_{50} values with **G1H4** improved by a factor of 2–4 compared with **G1H3**, and ≥ 10 times compared with **G1H2** and **G1H1** (Figure 4a and Table S1 in the Supporting Information). The only exception from this trend was observed at $EC_{50}<10$ μM, at which the onset of stoichiometric binding processes obscured intrinsic differences between individual transport systems.[56] As an interesting consequence, the activity of tetrabutyl octopus amphiphile **G1H4O4** was observable below the $EC_{50}=100$ μM threshold, whereas the corresponding **G1H3O4**, **G1H2O4** and **G1H1O4** were at $EC_{50}>100$ μM or fully inactive (Figure 4a, -----).

The increasing efficiency of octopus amphiphiles with increasing number of tails is likely to originate from improved partitioning into the membrane. This interpretation was supported by low Y_{MAX} and low n with octopus amphiphiles from **G1H4** (Figure 4b and 4c). Low Y_{MAX} is commonly interpreted as an early onset of precipitation of overly hydrophobic transporter components during their delivery to the membrane at higher concentrations. However, Y_{MAX} never dropped below the 50% threshold except for **G1H4O4** with an exceptionally low $Y_{MAX}=(14.9\pm1.0)\%$ (Figure 4b, -----). Decreasing n with increasing number and length of hydrophobic tails revealed increasing stability of the final polyion–counterion transporters under these conditions.[55] Maximal $n=6$–9 indicated that the binding of at least 6–9 counterions is needed to activate ctDNA transporters. Minimal $n>2$ remained far above the $n=1$ threshold. This demonstrated that also the most stable transport system is thermodynamically unstable. As highly dynamic minority components, all active structures are thus undetectable by routine spectroscopic methods (Figure 4c, -----).[55,56]

Detection and discrimination of anisaldehyde odorants **O11**–**O13** was one of the problems faced with the previously reported reactive cations **G1H1**–**G1H3** and **A1H1**–**A1H3** (Figure 5, ——). This problem was rationalized with insufficient amphiphilicity. With octopus amphiphiles obtained from peptide dendron **G1H4**, activities increased approximately 3 times with a lowest $EC_{50}=(4.3\pm0.8)$ μM for the *meta* isomer **O12**. Consistently weaker activity with the *ortho* isomer **O11** and *para* isomer **O13** could possibly originate from incomplete hydrazone formation because of their reduced electrophilicity (or from steric effects in the final amphiphiles, etc.).

Enantiodiscrimination is of critical importance in all sensing systems. With fragrance sensors, (*R*)-(−)-muscone **O1** represents a benchmark challenge concerning enantiodiscri-

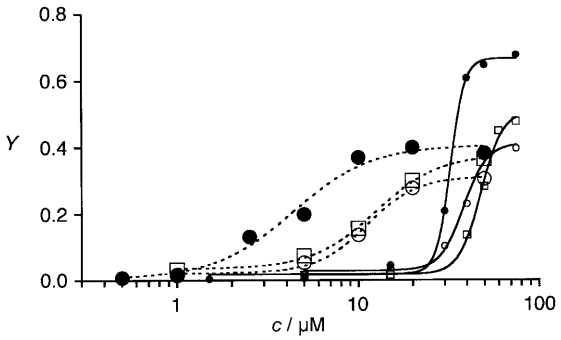

Figure 5. Dose-response curves for DNA activation by guanidinium hydrazides **G1H4** (-----) and **G1H3** (——) after incubation with *o*-anisaldehyde **O11** (○), *m*-anisaldehyde **O12** (●), and *p*-anisaldehyde **O13** (□). Data for **G1H3** are adapted from ref. [27]; for details, compare Figure 2 and the Supporting Information.

mination. Muscone is extracted from a glandular secretion by musk deer, and has been used for centuries in perfumery and medicine.[57] Discrimination of enantioenriched (*R*)-(−)-muscone **O1** (61% *ee*) and racemic (±)-muscone **O2** with the previous trihydrazide countercation **G1H3** and ctDNA transducers was not clear considering the similarity of their EC_{50} values of (23.0±2.1) and (33.6±4.2) μM, respectively, and their Y_{MAX} (Figure 6a, □). In this case, reliable discrimination was possible only by differential sensing by using pattern generation with **G1H2**, **G1H3**, **A1H2**, and **A1H3**, and pattern analysis with standard PCA or hierarchical clustering analysis (HCA) methods.

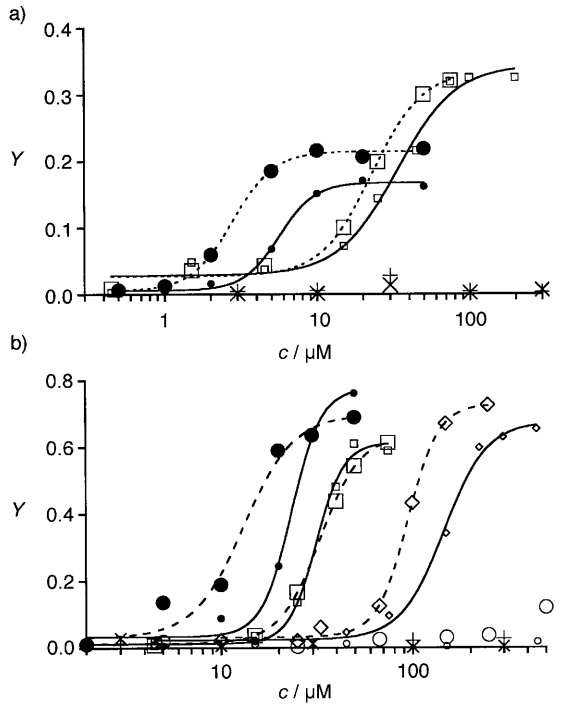

Figure 6. a) Dose-response curves for (−)-muscone **O1** (-----) and (±)-muscone **O2** (——) derivatized with **G1H3** (□) and **G1H4** (●); **O1** (×) and **O2** (+) alone were also measured. b) Dose-response curves for (−)-carvone **O9** (——) and (+)-carvone **O10** (-----) derivatized with **G1H4** (●), **G1H3** (□), **G1H2** (◇) and **G1H1** (○); **O9** (×) and **O10** (+) alone were also measured. Data for **G1H3**, **G1H2**, and **G1H1** are adapted from ref. [27]; for details, compare Figure 2 and the Supporting Information.

Attached to peptide dendrons, each 15-membered ring of muscone appears to contribute two alkyl tails to the octopus amphiphiles that are linked together at the end (Figure 1). In amphiphile **G1H4O1**, this adds up to eight tails in total. As a result, minor structural differences are multiplied in octopus amphiphiles. For instance, the number of stereogenic centers raises from one in muscone and five in amphiphile **G1H3O1** to seven in octopus amphiphile **G1H4O1**. This enhanced chirality suggests that octopus amphiphiles should be ideal to enable enantiodiscrimination. Compared with **G1H3**, the effective concentrations obtained for muscone with **G1H4** improved almost 10 times to $EC_{50}=(2.8\pm0.1)$ and (5.6±0.3) μM (Figure 6a, ●). Together with clearer differences in Y_{MAX}, the dose-response curves for enantioenriched (−)-muscone **O1** (Figure 6a, ●, -----) and racemic (±)-muscone **O2** (Figure 6a, ●, ——) became distinguishable without PCA or HCA treatment. Because of high hydrophobicity leading to inefficient delivery, the absolute Y_{MAX} of fragrant octopus amphiphiles **G1H4O1** and **G1H4O2** became, however, disappointingly low.

The ability of octopus amphiphiles to enable enantiodiscrimination was very satisfactory with carvone, the leading example for ring-contracted monoterpene analytes.[58] Attached to minidendron **G1H3**, the two enantiomers produced essentially the same dose-response curve at an intermediate $EC_{50}=31$–33 μM (Figure 6b, □). Attached to the expanded peptide dendron **G1H4**, both efficiency and discrimination power improved to an excellent $EC_{50}=(13.2\pm1.6)$ μM for **G1H4O9** and $EC_{50}=(23.5\pm1.3)$ μM for **G1H4O10** without any complementary cuts in Y_{MAX} (Figure 6b, ●).

To estimate the increase in enantiodiscriminatory power mediated by octopus amphiphiles obtained from **G1H4** more quantitatively, HCA was applied to the minimalist pattern produced by all obtained Hill parameters measured with **G1H3** and **G1H4** for muscones and carvones. HCA is an unsupervised method of multivariant analysis that converts all interpoint Euclidean distances in multidimensional patterns into 2D dendrograms. The significant shortest distances in these dendrograms, measured in Eucliden units (E.u.), can be cautiously used as a semiquantitative indication of sensing power. In the HCA dendrogram obtained with **G1H3** only, the carvone enantiomers were separated by 26 E.u., whereas the enantiomer mixtures of muscone were separated by 12 E.u. (Figure 7a). In the HCA dendrogram produced by **G1H3** and **G1H4**, the carvone enantiomers were separated by 44 E.u., whereas enantiodiscrimination of muscones increased more than 3 times to 38 E.u. (Figure 7b).

Compared with the many elegant, often much more practical differential chemosensors reported over the past two decades,[28–46] sensing systems that work in lipid bilayers are of interest because subtle differences in structure are magnified by covalent capture of several analytes by the same

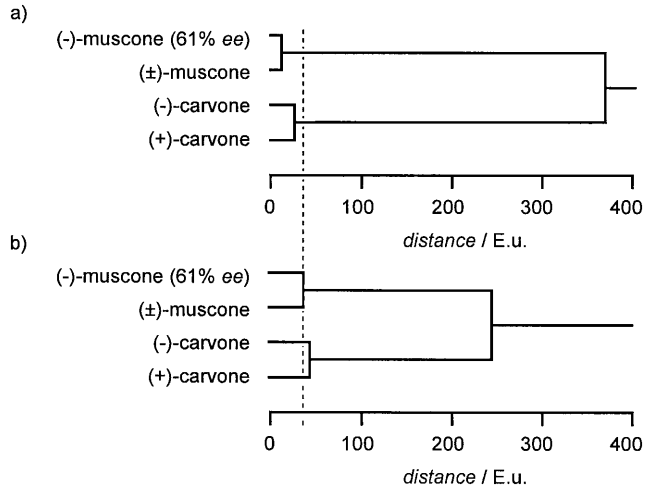

Figure 7. HCA dendrogram showing the Euclidian distances between average values for data obtained with: a) **G1H3**, and b) **G1H3** and **G1H4**; dotted line: 40 E.u.

counterion head-group and by the noncovalent assembly of multiple counterion activators on one polyion transporter. This is particularly true for the discrimination of enantiomeric analytes, for which these effects are expressed in a chiral environment. Covalent capture of pairs of enantiomers as analytes by chiral counterions produces diastereomeric amphiphilies, which will in turn interact differently with chiral DNA transporters, and the resulting diastereomeric polyion–counterion complexes will interact differently with the chiral phospholipids in the membrane. This situation implies that chiral reactive counterions are not necessary to enable enantiodiscrimination. The different binding of enantiomeric amphiphiles to chiral polyions and membranes should suffice to discriminate enantiomeric analytes. However, increasing the number of stereogenic centers in and the number of chiral analytes attached to the reactive counterions should naturally increase enantiodiscrimination. The reported results with octopus amphiphile **G1H4** are in agreement with this interpretation.

Conclusion

The general conclusion of this study is simple but attractive for several reasons. Cationic hydrazone amphiphiles with four hydrophobic tails are the most powerful activators of DNA transporters in lipid bilayers known today. Moreover, increasing activity and discriminatory power with increasing number of tails is confirmed. The emergence of stoichiometric binding with more hydrophobic analytes suggests that octopus amphiphiles with one head and four tentacles could be nearly ideal (Figure 3a). Preliminary results are in agreement with the expectation that efficiencies are unlikely to further increase with more than four analytes per amphiphile.

The high activator efficiency found for octopus amphiphiles is particularly interesting with regard to cellular uptake.[49–54] RNAi, for example, which is a general approach to regulate gene expression, operates with short oligonucleotides, that is, siRNA that show less pronounced multivalency effects and can thus respond less convincingly to more conventional amphiphiles.[59] Moreover, dynamic octopus amphiphiles would be interesting to mix in a fluorescent probe to image uptake pathways[52–54] or membrane domains[60] without significantly disturbing intrinsic function.

Experimental Section

Details of all experimental procedures and characterizations can be found in the Supporting Information.

Acknowledgements

We thank A. Hennig for help with data analysis, D. Jeannerat, A. Pinto, and S. Grass for NMR measurements, G. Hopfgartner, S. Michalet, P. Perrottet, and N. Oudry for MS measurements, L. Wunsche and A. Herrmann (Firmenich, Geneva) for odorant samples, and the University of Geneva and the Swiss NSF for financial support.

[1] L. B. Buck, *Angew. Chem.* **2005**, *117*, 6283–6296; *Angew. Chem. Int. Ed.* **2005**, *44*, 6128–6140.
[2] G. Das, S. Matile, *Chem. Eur. J.* **2006**, *12*, 2936–2944.
[3] S. Matile, H. Tanaka, S. Litvinchuk, *Top. Curr. Chem.* **2007**, *277*, 219–250.
[4] N. Sakai, J. Mareda, S. Matile, *Acc. Chem. Res.* **2008**, *41*, 1354–1365.
[5] S. Matile, A. Som, N. Sordé, *Tetrahedron* **2004**, *60*, 6405–6435.
[6] A. L. Sisson, M. R. Shah, S. Bhosale, S. Matile, *Chem. Soc. Rev.* **2006**, *35*, 1269–1286.
[7] J. T. Davis, P. A. Gale, O. A. Okunola, P. Prados, J. C. Iglesias-Sanchez, T. Torroba, R. Quesada, *Nat. Chem.* **2009**, *1*, 138–144.
[8] R. J. Brea, C. Reiriz, J. R. Granja, *Chem. Soc. Rev.* **2010**, *26*, 1448–1456.
[9] M. Febles, N. Pérez-Hernandez, C. Pérez, M. L. Rodríguez, C. Foces-Foces, M. V. Roux, E. Q. Morales, G. Buntkowsky, H. H. Limbach, J. D. Martín, *J. Am. Chem. Soc.* **2006**, *128*, 10008–10009.
[10] T. M. Fyles, *Chem. Soc. Rev.* **2007**, *36*, 335–347.
[11] A. P. Davis, D. N. Sheppard, B. D. Smith, *Chem. Soc. Rev.* **2007**, *36*, 348–357.
[12] G. W. Gokel, N. Barkey, *New J. Chem.* **2009**, *33*, 947–963.
[13] C. P. Wilson, S. J. Webb, *Chem. Commun.* **2008**, 4007–4009.
[14] A. Satake, M. Yamamura, M. Oda, Y. Kobuke, *J. Am. Chem. Soc.* **2008**, *130*, 6314–6315.
[15] X. Li, B. Shen, X. Q. Yao, D. Yang, *J. Am. Chem. Soc.* **2009**, *131*, 13676–13680.
[16] M. Jung, H. Kim, K. Baek, K. Kim, *Angew. Chem.* **2008**, *120*, 5839–5841; *Angew. Chem. Int. Ed.* **2008**, *47*, 5755–5757.
[17] P. L. Boudreault, N. Voyer, *Org. Biomol. Chem.* **2007**, *5*, 1459–1465.
[18] N. Sakai, B. Baumeister, S. Matile, *ChemBioChem* **2000**, *1*, 123–125.
[19] N. Sakai, S. Matile, *J. Am. Chem. Soc.* **2003**, *125*, 14348–14356.
[20] T. Takeuchi, V. Bagnacani, F. Sansone, S. Matile, *ChemBioChem* **2009**, *10*, 2793–2799.
[21] G. Das, P. Talukdar, S. Matile, *Science* **2002**, *298*, 1600–1602.
[22] T. Miyatake, M. Nishihara, S. Matile, *J. Am. Chem. Soc.* **2006**, *128*, 12420–12421.
[23] S. Litvinchuk, N. Sordé, S. Matile, *J. Am. Chem. Soc.* **2005**, *127*, 9316–9317.
[24] S. Litvinchuk, H. Tanaka, T. Miyatake, D. Pasini, T. Tanaka, G. Bollot, J. Mareda, S. Matile, *Nat. Mater.* **2007**, *6*, 576–580.

[25] S. M. Butterfield, T. Miyatake, S. Matile, *Angew. Chem.* **2009**, *121*, 331–334; *Angew. Chem. Int. Ed.* **2009**, *48*, 325–328.
[26] T. Takeuchi, S. Matile, *J. Am. Chem. Soc.* **2009**, *131*, 18048–18049.
[27] T. Takeuchi, J. Montenegro, A. Hennig, S. Matile, *Chem. Sci.* DOI: 10.1039/c0sc00386g.
[28] J. J. Lavigne, E. V. Anslyn, *Angew. Chem.* **2001**, *113*, 3212–3225; *Angew. Chem. Int. Ed.* **2001**, *40*, 3118–3130.
[29] M. A. Palacios, R. Nishiyabu, M. Marquez, P. Anzenbacher, Jr., *J. Am. Chem. Soc.* **2007**, *129*, 7538–7544.
[30] J. R. Epstein, D. R. Walt, *Chem. Soc. Rev.* **2003**, *32*, 203–214.
[31] C. Zhang, K. S. Suslick, *J. Am. Chem. Soc.* **2005**, *127*, 11548–11549.
[32] H. Zhou, L. Baldini, J. Hong, A. J. Wilson, A. D. Hamilton, *J. Am. Chem. Soc.* **2006**, *128*, 2421–2425.
[33] A. Buryak, K. Severin, *J. Am. Chem. Soc.* **2005**, *127*, 3700–3701.
[34] S. H. Shabbir, L. A. Joyce, G. M. da Cruz, V. M. Lynch, E. Sorey, E. V. Anslyn, *J. Am. Chem. Soc.* **2009**, *131*, 13125–13131.
[35] J. C. Jurs, G. A. Bakken, H. E. McClelland, *Chem. Rev.* **2000**, *100*, 2649–2678.
[36] J. W. Lee, J.-S. Lee, Y.-T. Chang, *Angew. Chem.* **2006**, *118*, 6635–6637; *Angew. Chem. Int. Ed.* **2006**, *45*, 6485–6487.
[37] D. C. Gonzlez, E. N. Savariar, S. Thayumanavan, *J. Am. Chem. Soc.* **2009**, *131*, 7708–7716.
[38] O. R. Miranda, H.-T. Chen, C.-C. You, D. E. Mortenson, X.-C. Yang, U. H. F. Bunz, V. M. Rotello, *J. Am. Chem. Soc.* **2010**, *132*, 5285–5289.
[39] N. T. Greene, K. D. Shimizu, *J. Am. Chem. Soc.* **2005**, *127*, 5695–5700.
[40] *Topics in Current Chemistry, Vol. 277* (Ed.: T. Schrader), Springer, Heidelberg, **2007**.
[41] C. Guarise, L. Pasquato, V. De Filippis, P. Scrimin, *Proc. Natl. Acad. Sci. USA* **2006**, *103*, 3978–3982.
[42] A. Wada, S. Tamaru, M. Ikeda, I. Hamachi, *J. Am. Chem. Soc.* **2009**, *131*, 5321–5330.
[43] T. D. James, *Top. Curr. Chem.* **2007**, *277*, 107–154.
[44] R. Jelinek, S. Kolusheva, *Top. Curr. Chem.* **2007**, *277*, 155–180.
[45] L. Vial, P. Dumy, *New J. Chem.* **2009**, *33*, 939–946.
[46] M. Florea, W. M. Nau, *Org. Biomol. Chem.* **2010**, *8*, 1033–1039.
[47] K. Sadler, J. P. Tam, *Rev. Mol. Biotechnol.* **2002**, *90*, 195–229.
[48] T. Darbre, J.-L. Reymond, *Acc. Chem. Res.* **2006**, *39*, 925–934.
[49] D. A. Tomalia, A. M. Naylor, W. A. Goddard, *Angew. Chem.* **1990**, *102*, 119–157; *Angew. Chem. Int. Ed. Engl.* **1990**, *29*, 138–175.
[50] M. Liu, J. M. J. Frechet, *Pharm. Sci. Technol. Today* **1999**, *2*, 393–401.
[51] K. T. Al-Jamal, T. Sakthivel, A. T. Florence, *Coll. Surface A: Phys. Eng. Asp.* **2005**, *268*, 52–59.
[52] S. Bhattacharya, A. Bajaj, *Chem. Commun.* **2009**, 4632–4656.
[53] J. Fernández-Carneado, M. Van Gool, V. Martos, S. Castel, P. Prados, J. de Mendoza, E. Giralt, *J. Am. Chem. Soc.* **2005**, *127*, 869–874.
[54] T. Takeuchi, M. Kosuge, A. Tadokoro, Y. Sugiura, M. Nishi, M. Kawata, N. Sakai, S. Matile, S. Futaki, *ACS Chem. Biol.* **2006**, *1*, 299–303.
[55] S. Bhosale, S. Matile, *Chirality* **2006**, *18*, 849–856.
[56] F. Mora, D.-H. Tran, N. Oudry, G. Hopfgartner, D. Jeannerat, N. Sakai, S. Matile, *Chem. Eur. J.* **2008**, *14*, 1947–1953.
[57] L. Ruzicka, *Helv. Chim. Acta* **1926**, *9*, 715–729.
[58] G. Wagner, *Chem. Ber.* **1894**, *27*, 2270–2276.
[59] A. Fire, S. Xu, M. Montgomery, S. Kostas, S. Driver, C. Mello, *Nature* **1998**, *391*, 806–811.
[60] L. A. Bagatolli, *Biochim. Biophys. Acta.* **2006**, *1758*, 1541–1556.

Received: September 9, 2010
Published online: October 29, 2010

